Digital Filter and Square Timing Recovery

MARTIN OERDER, STUDENT MEMBER, IEEE, AND HEINRICH MEYR, FELLOW, IEEE

Abstract—**Digital realizations of timing recovery circuits for digital data transmission are of growing interest. In this paper, we present a new digital algorithm which can be implemented very efficiently also at high data rates. The resulting timing jitter has been computed and verified by simulations. In contrast to other known algorithms, the one presented here allows free running sampling oscillators and a new planar filtering method which prevents synchronization hangups.**

I. Introduction

Digital realizations of receivers for synchronous data signals—baseband as well as QPSK or QAM signals—are of growing interest as the capabilities of signal processors (for low data rates) and application specific integrated circuits (for high data rates) increase. These receivers have to include algorithms for timing recovery. Several such discrete-time algorithms have been proposed during the last few years [1]–[3]. The majority of these solutions, however, include only the integration of one part of the timing synchronization, namely, the generation of some kind of timing error signal, into the digital part of the receiver. This error signal is then typically used to control an analog VCO which generates the sampling strobes.

Due to the advantages of an integrated realization, however, as much of the receiver as possible should be digital. This means that the input signal should be sampled at a fixed rate by a free running oscillator and all further processing should then be done digitally using these samples. For symbol detection, this means that the optimum decision metrics must be generated from the given samples by some sort of interpolation which is controlled by an estimate of the current timing offset [4]. Therefore, we need an algorithm which determines this absolute timing offset (not only a timing error signal) from the given samples of the signal.

Such an algorithm is proposed in this paper. It is the digital counterpart of the well-known continuous-time filter and square timing recovery [5], [6], but it extracts the timing information from the squared signal in a new way. The analysis of the timing jitter presented in this paper leads to results that are similar to the continuous-time case, although the method of analysis is different.

Another main contribution of the paper is a new method of hangup-free filtering of the timing signal. With all other known timing recovery methods a major problem is that the synchronization loop can get stuck at an unstable equilibrium point. In this paper, we show how this can be avoided through planar filtering of two-dimensional timing estimates.

The final section of the paper presents a digital realization of the timing detector which is suitable for VLSI integration also at high data rates.

Paper approved by the Editor for Signal Design, Modulation, and Detection of the IEEE Communications Society. Manuscript received April 18, 1987; revised September 23, 1987. This paper was presented at GLOBECOM '87, Tokyo, Japan, November 1987.

The authors are with Lehrstuhl für Elektrische Regelungstechnik, Aachen University of Technology, West Germany.

IEEE Log Number 8820399.

II. Timing Estimation

Here we consider the timing recovery for digital data transmission by linear modulation schemes (PAM, QAM, PSK). The received signal (PAM) or the equivalent low-pass signal (QAM, PSK) can be written as

$$r(t)=\sum_{n=-\infty}^{\infty} a_n g_T(t-nT-\epsilon(t)T)+n(t)$$
$$=u(t)+n(t). \tag{1}$$

Where a_n are the complex valued transmitted symbols with mean power 1 (e.g., ± 1, $\pm i$ with QPSK), $g_T(t)$ is the transmission signal pulse, T is the symbol duration, $n(t)$ is the channel noise which is assumed to be white and Gaussian with power density N_0, and $\epsilon(t)$ is an unknown, slowly varying time delay.

Now timing recovery means the estimation of the delay $\epsilon(t)$ to enable the optimal detection of the data. Because ϵ varies very slowly, in a digital realization, we can process the received signal section by section. For each section Δ_m, we can assume ϵ to be constant and obtain an estimate $\hat{\epsilon}_m$. This estimate must then be combined with the previous estimates (i.e., it must be filtered) such that the optimal estimate $\bar{\epsilon}_m$ is obtained. The latter can be used to control an analog or digital sampler for the detection.

Below we consider a special type of timing estimator which is particularly suited for digital realization. It is similar to the continuous-time filter and square synchronizer in that the input signal is squared and the resulting spectral component at the symbol rate is extracted by a filtering operation. In Fig. 1 the algorithm is shown. After a receiving filter [impulse response $g_R(t)$] the signal $\tilde{r}(t) = r(t) * g_R(t)$ is sampled at rate N/T ("$*$" denotes a convolution). We thus have samples

$$\tilde{r}_k=\tilde{r}(kT/N). \tag{2}$$

The sequence

$$x_k=\left|\sum_{n=-\infty}^{\infty} a_n g\left(\frac{kT}{N}-nT-\epsilon T\right)+\tilde{n}\left(\frac{kT}{N}\right)\right|^2 \tag{3}$$

with

$$g(t)=g_T(t) * g_R(t)$$

represents the samples of the filtered and squared input signal and contains a spectral component at $1/T$. This spectral component, which in a conventional synchronizer is extracted by a PLL or a narrow-band filter is here determined for every section of length LT (i.e., from LN samples) by computing the complex Fourier coefficient at the symbol rate

$$X_m=\sum_{k=mLN}^{(m+1)LN-1} x_k e^{-j2\pi k/N}. \tag{4}$$

As is shown in the next section, the normalized phase $\hat{\epsilon}_m = -1/2\pi \arg(X_m)$ of this coefficient is an unbiased estimate for ϵ.

0090-6778/88/0500-0605$01.00

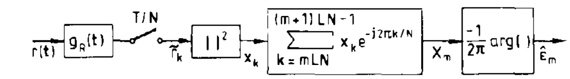

Fig. 1. Discrete-time filter and square estimator.

The sampling rate must be such that the spectral component at $1/T$ can still be represented, i.e., $N/T > 2/T$. We use $N = 4$ for practical reasons. In the case of bandwidth efficient modulation with a single-sided bandwidth of less than $1/T$, the receiving filter $g_R(t)$ also has a single-sided bandwidth of less than $1/T$ and thus the squared signal has a single-sided bandwidth of less than $2/T$. Therefore, with $N = 4$, the sequence x_k completely describes the underlying continuous-time signal.

III. Statistics of the Estimate

In this section, we compute the statistics of the estimate $\hat{\epsilon}_m$ as a function of the pulse form $g(t)$ and the noise power density N_0 of the additive noise. We assume $m = 0$ and omit the index m for the sake of simpler notation.

A. Mean

The mean of the estimate is

$$E[\hat{\epsilon}] = E\left[\frac{-1}{2\pi}\arg(X)\right]. \tag{5}$$

For small variance of the estimates we can linearize the arg-operation.

$$\begin{aligned} E[\hat{\epsilon}] &\approx \frac{-1}{2\pi}\arg(E[X]) \\ &= \frac{-1}{2\pi}\arg\left(\sum_{k=0}^{LN-1} E[x_k]e^{-j2\pi k/N}\right). \end{aligned} \tag{6}$$

The linearization is valid, of course, only for $|\arg(X)| \ll \pi$. However, due to the subsequent filter operations, which are discussed in Section IV, this is the only case of interest.

We first have to compute the expectation of the squared signal

$$E[x_k] = E\left[\left|\sum_{n=-\infty}^{\infty} a_n g(kT/N - nT - \epsilon T) + \tilde{n}(kT/N)\right|^2\right]. \tag{7}$$

The expectation must be taken with respect to the joint distribution of the symbols a_n and the noise $n(t)$. Noise and symbols are independent of each other. Therefore, and with $E[\tilde{n}(t)] = 0$, the cross term of the binomial in (7) vanishes. The remaining terms are

$$\begin{aligned} E[x_k] &= E\left[\left|\sum_{n=-\infty}^{\infty} a_n g(kT/N - nT - \epsilon T)\right|^2\right] \\ &\quad + E[|\tilde{n}(kT/N)|^2] \\ &= \sum_{n=-\infty}^{\infty}\sum_{m=-\infty}^{\infty} E[a_n a_m^*] g(kT/N - nT - \epsilon T) \\ &\quad \cdot g^*(kT/N - mT - \epsilon T) + E[|\tilde{n}(kT/N)|^2]. \end{aligned} \tag{8}$$

With noise power σ^2 and independently distributed symbols of mean power 1, we have

$$E[x_k] = \sum_{n=-\infty}^{\infty} |g(kT/N - nT - \epsilon T)|^2 + \sigma^2. \tag{9}$$

Using the identity (A6) from Appendix A, we obtain for tl expectation of X

$$E[X] = \sum_{k=0}^{LN-1} E[x_k]e^{-j2\pi k/N} \qquad (1$$

$$= \frac{LN}{T}\mathfrak{F}[|g(t-\epsilon T)|^2]_{f=1/T} \qquad (1$$

with

$$\mathfrak{F}[x(t)] = \int_{-\infty}^{\infty} x(t)e^{-j2\pi ft}\,dt.$$

At this point, we introduce the following functions to simpli the notation:

$$p_n(t) = g(t)g^*(t-nT) \qquad (1$$

$$P_n(f) = \mathfrak{F}[p_n(t)]. \qquad (1$$

We then have

$$\begin{aligned} E[X] &= \frac{LN}{T}\mathfrak{F}[p_0(t-\epsilon T)]_{f=1/T} \\ &= \frac{LN}{T}P_0(1/T)e^{-j2\pi\epsilon} \end{aligned} \qquad (1$$

and thus

$$\begin{aligned} E[\hat{\epsilon}] &= \frac{-1}{2\pi}\arg\left(\frac{LN}{T}P_0(1/T)e^{-j2\pi\epsilon}\right) \\ &= \epsilon - \frac{1}{2\pi}\arg P_0(1/T). \end{aligned} \qquad (1$$

Therefore, under the assumption

$$\arg P_0(1/T) = 0, \qquad (1$$

$\hat{\epsilon}$ is an unbiased estimate of the clock phase ϵ. But even if (1 is not valid, the mean of $\hat{\epsilon}$ exactly equals the required sampli offset as we show below. We assume

$$g_R(t) = g_T^*(-t + \alpha T) \quad \text{(generalized matched filter).} \qquad (1$$

We then have

$$g(t) = g_0(t - \alpha T) \quad \text{with } g_0(t) = g_T(t) * g_T^*(-t) \qquad (1$$

$$\tilde{r}(t) = \sum_n a_n g_0(t - nT - \epsilon T - \alpha T) + \tilde{n}(t). \qquad ($$

Since $g_0(t)$ is symmetrical, the optimal sampling instant is $g_0(t = 0)$, i.e., for the symbol a_n at

$$t_{\text{opt},n} = nT + \epsilon T + \alpha T, \qquad ($$

i.e., the required sampling offset is $(\epsilon + \alpha)T$. Evaluating (then yields

$$P_0(f) = e^{-j2\pi\alpha Tf}\mathfrak{F}[g_0(t)g_0^*(t)]. \qquad ($$

Since $g_0(t)$ is symmetrical, the Fourier transform in (21) real.

Therefore, we have

$$\arg P_0(1/T) = -2\pi\alpha \qquad ($$

and thus

$$E[\hat{\epsilon}] = \epsilon + \alpha \qquad ($$

which is exactly what is required for symbol detection.

B. Variance

Here we determine the variance of the random variable $\hat{\epsilon}$, i.e., the mean square error of the estimation. We assume

$$\epsilon = 0$$
$$\arg P_0(1/T) = 0 \tag{24}$$

to simplify the notation. (It can easily be shown that the results are valid for arbitrary ϵ and $\arg P_0$.) We then have

$$\begin{aligned}\mathrm{var}\,[\hat{\epsilon}] &= E[\hat{\epsilon}^2] \\ &= \frac{1}{(2\pi)^2} E\,[(\arg(X))^2] \\ &\approx \frac{1}{(2\pi)^2} \frac{E\,[(\mathrm{Im}\,X)^2]}{(E\,[\mathrm{Re}\,X])^2}.\end{aligned} \tag{25}$$

The latter approximation is valid since the imaginary part of X has zero mean and the variances of both imaginary and real part are small compared to the squared real mean.

From (14) and (24) follows

$$E\,[\mathrm{Re}\,X] = E[X] = \frac{LN}{T} P_0(1/T). \tag{26}$$

The variance of the imaginary part is

$$\begin{aligned}&E\,[(\mathrm{Im}\,X)^2] \\ &= E\left[\left(\mathrm{Im}\left[\sum_{k=0}^{LN-1} x_k e^{-j2\pi k/N}\right]\right)^2\right] \\ &= \sum_{k'=0}^{LN-1}\sum_{k=0}^{LN-1} E[x_k x_{k'}]\sin(2\pi k/N)\sin(2\pi k'/N)\end{aligned} \tag{27}$$

with

$$x_k = \left|\sum_{n=-\infty}^{\infty} a_n g(kT/N - nT) + \tilde{n}(kT/N)\right|^2. \tag{28}$$

By using some approximations which are valid for large L, the expectation can be computed (Appendix B). If the results are used in (25), we obtain

$$\mathrm{var}\,[\hat{\epsilon}] = \sigma^2_{s\times s} + \sigma^2_{s\times n} + \sigma^2_{n\times n} \tag{29}$$

with

$$\sigma^2_{s\times s} = \frac{1}{(2\pi)^2}\frac{1}{L}\frac{\sum_m (\mathrm{Im}\,P_m(1/T))^2}{(P_0(1/T))^2} \tag{30a}$$

$$\sigma^2_{s\times n} = \frac{1}{(2\pi)^2}\frac{1}{L} N_0 \frac{2I_3}{(P_0(1/T))^2} \tag{30b}$$

$$\sigma^2_{n\times n} = \frac{1}{(2\pi)^2}\frac{1}{L} N_0^2 \frac{\frac{T}{2}\mathrm{Re}\,\Phi(1/T)}{(P_0(1/T))^2} \tag{30c}$$

$$I_3 = \int_{-\infty}^{\infty}\int_{-\infty}^{\infty} g(t)g^*(t')\varphi(t-t') \cdot \sin(2\pi t/T)\sin(2\pi t'/T)\,dt\,dt' \tag{31}$$

$$\Psi(f) = \mathfrak{F}[\varphi^2(t)] \tag{32}$$

$$\varphi(\tau) = \int_{-\infty}^{\infty} g_R(t) g_R^*(t+\tau)\,dt. \tag{33}$$

The three terms [30a)–c)] represent the parts of the timing jitter that are generated by (signal $\times$ signal), (signal $\times$ noise), and (noise $\times$ noise) interaction.

C. Conditions for Asymptotically Jitter-Free Timing Recovery

In this section, we study the conditions to be fulfilled by the transmit and receive filters necessary for the timing estimate to have zero variance in the noiseless case ($N_0 = 0$), i.e., the conditions for the $s \times s$-portion of the variance

$$\sigma^2_{s\times s} = \frac{1}{(2\pi)^2}\frac{1}{L}\frac{\sum_m (\mathrm{Im}\,P_m(1/T))^2}{(P_0(1/T))^2} \tag{34}$$

to be zero.

We have

$$p_m(t) = g(t)g^*(t-mT) \tag{35}$$

$$\begin{aligned}P_m(f) &= G(f) * (G^*(-f)e^{-j2\pi f mT}) \\ &= \int_{-\infty}^{\infty} G(f-\nu)G^*(-\nu)e^{-j2\pi\nu mT}\,d\nu\end{aligned} \tag{36}$$

and use of the abbreviation

$$H(f) = G(1/T - f)G^*(-f) \tag{37}$$

yields

$$P_m(1/T) = \int_{-\infty}^{\infty} H(\nu)e^{-j2\pi\nu mT}\,d\nu. \tag{38}$$

For real valued $g(t)$, i.e., symmetrical joint transfer function of the transmit and the receive filter, we have

$$G^*(-f) = G(f) \tag{39}$$

$$H(f) = G(1/T - f)G(f). \tag{40}$$

That means that $H(f)$ is symmetrical around $1/2T$ and

$$\mathrm{Im}\,P_m(1/T) = \int_{-\infty}^{\infty} \mathrm{Im}\,H(\nu)\cos(2\pi\nu mT)\,d\nu. \tag{41}$$

Therefore, a sufficient condition for zero jitter is

$$\mathrm{Im}\,H(f) = 0 \tag{42}$$

which can be obtained, for example, with

$$g(t) = g(-t) \quad \text{(symmetrical pulse shape)} \tag{43}$$

and also of course with all linear-phase pulses

$$g(\tau + t) = g(\tau - t) \tag{44}$$

as they act like the corresponding symmetrical pulse $g(t - \tau)$ with an additional timing delay $\epsilon_0 = \tau$. The conditions (43) and (44), however, show that the optimal receive filter in the synchronization path is a matched filter

$$g_R(t) = g_T(-t). \tag{45}$$

These results are valid, of course, only with the approximations made in Section III-B, in particular, only for large estimation intervals LT. In the case of short intervals, the estimate exhibits jitter, but the spectrum of the jitter has a zero at the origin and can thus be suppressed by low-pass filtering. True absence of jitter can be obtained in general only by using nonoverlapping pulses.

This is in contrast to the conventional continuous-time filter and square timing recovery. In the continuous-time case, the timing is determined by detecting the zeros of the timing wave.

Therefore, true jitter-free timing recovery is possible if the timing wave exhibits only amplitude jitter, but no phase jitter. The latter can be achieved, for example, with locally symmetric pulses [7]. In our case, however, the estimation is based on samples which have an arbitrary offset from the zeros and thus exhibit random amplitude fluctuations. Therefore, only asymptotically jitter-free recovery can be obtained.

D. Simulation Results

Fig. 2 shows the variance of the estimates $\hat{\epsilon}$ (29) for several estimation intervals L where both transmit and receive filter are fourth-order Butterworth filters with corner frequency $0.7/T$ and the modulation format is 8PSK (solid lines). The markers show the results of Monte Carlo simulations (5000 estimates for each point). In addition, for $L = 64$, the three parts of (29) are shown by the dotted lines. The simulations are very close to the theoretical results. Only for $L < 4$ are there errors due to the approximations in the computation of the variance which are valid for large L only. For $L = 1$ and $E/N_0 = 0$ dB the simulation result is smaller than the theoretical result. This is due to the finite range of ϵ. The variance tends to 1/12 when $\hat{\epsilon}$ is uniformly distributed in the estimation range.

Fig. 3 shows the corresponding curves for linear phase filters with a transfer function amplitude similar to the above Butterworth filter. For $L \geq 16$ and with moderate E/N_0 the simulation results match the theory very well. In particular, the predicted missing of an $s \times s$-portion of the variance can be seen. Because the absolute variances are much smaller than in Fig. 2, the effects of the finite observation intervals LT are much more visible here, especially for large E/N_0.

E. Frequency Offset

Since we use a free running sampling oscillator, a frequency offset between transmit and receive timing may be present resulting in a continuously rising or falling ϵ. In contrast to carrier recovery, however, the frequency offset in timing recovery is very small ($10^{-5} \cdots 10^{-2}$ of the symbol rate). We can therefore always find an observation length $L = L'$ for which we can consider ϵ to be approximately constant. Then all considerations of the previous sections apply. For $L > L'$ inspection of the estimation algorithm reveals that the estimate X is nothing but the average over estimates from shorter intervals. Therefore, also the mean of the estimate $\hat{\epsilon}$ is just the average of the timing delay ϵ over the observation interval, as long as the variation of ϵ is smaller than $T/2$. The latter condition, of course, limits the possible observation length L.

Similarly, for small frequency offsets, the variance of the estimates can be expected to be nearly independent of the frequency offset. For larger frequency offsets, one would have to examine whether the algorithm behaves like its continuous-time counterpart that exhibits a significant increase in timing jitter in the presence of frequency offset.

IV. Planar Filtering of the Estimates

Due to frequency offset and random variations of the delay ϵ, the observation length L is limited. The estimation, however, can be significantly improved if the knowledge of the statistical properties of ϵ is used to postfilter the estimates. For example, a simple "random walk" model for the time delay ϵ leads to a first-order Kalman filter. The variance of the filtered estimates can be computed from the variance of the unfiltered estimates and the random walk parameters [8]. Since the range of the estimates $\hat{\epsilon}_m$ is finite, the filter innovation must be reduced to the range $[-0.5, 0.5]$ as shown in Fig. 4.

With this kind of filtering, however, the following situation can occur. If the true value ϵ is at a value 0.5 distant from the filtered value $\tilde{\epsilon}$, the estimates $\hat{\epsilon}$ also vary around this value and thus the innovation is at ± 0.5 and vanishes in the mean. Then

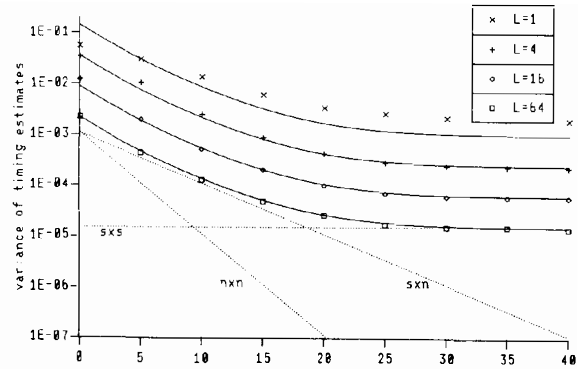

Fig. 2. Computed and simulated variance of the timing estimate for severa estimation intervals L. Transmit and receive filter are fourth-orde Butterworth, $f_c = 0.7/T$. Dotted lines: $s \times s$, $s \times n$, and $n \times n$-part fo $L = 64$.

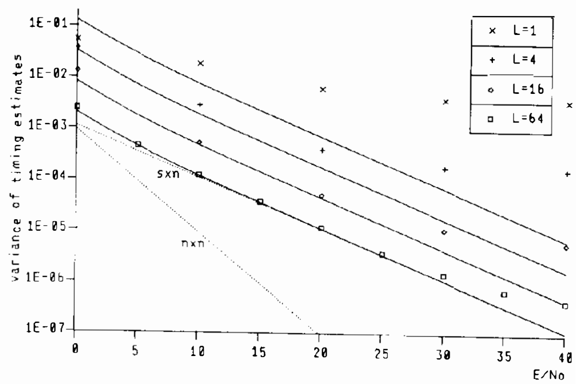

Fig. 3. As Fig. 2, but linear-phase filters.

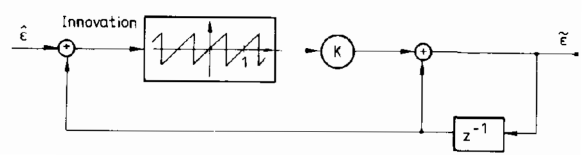

Fig. 4. Filtering of the estimates.

the filter is in an unstable equilibrium and it can remain ther some time in spite of the large error.

This is a problem which arises also for other models an filters and with almost all known synchronization methods even if they—like the one presented above—could be calle "open loop" at first sight. Because of the periodic behavior c the filtered delay "hangups" can occur in the filter loop.

Below we present a realization which avoids these prob lems. The central idea is to filter a complex phasor instead c the corresponding (periodic) angle. The term X_m from Fig. is such a phasor. Instead of first determining the angle of thi phasor and filtering the angle, we can apply a Kalman filter t the phasor itself and use the angle of the filtered phasor t control the sampling (Fig. 5).

In Figs. 6 and 7, a situation for filtering of ϵ and filtering c X is shown. In the first case a hangup can occur if the error i $\tilde{\epsilon}$ is approximately 0.5 (corresponding to an angle of π). Wit planar filtering, however, the filtered value $\tilde{X}$ moves correctl (with a step width which depends on the filter coefficient present) towards its place. Thus, hangup problems cannc occur any more.

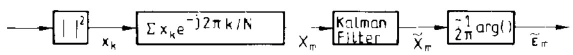

Fig. 5. Planar filtering of the estimates.

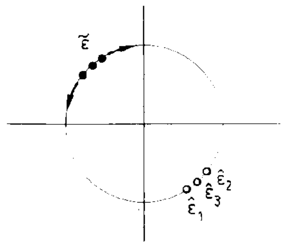

Fig. 6. Example for the trajectory of estimate and filtered value with filtering of the delay values.

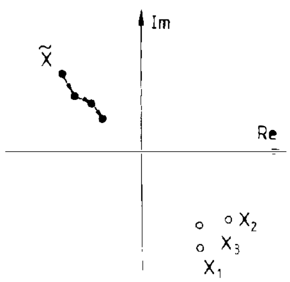

Fig. 7. Fig. 6, but planar filtering.

The filtered estimate $\tilde{\epsilon}_m$ of Fig. 5 has of course the finite range $[-0.5, 0.5]$ again and with only small variation in $\tilde{X}_m$ jumps can occur between ± 0.5 in $\tilde{\epsilon}_m$. The interpolation unit, however, which is controlled by $\tilde{\epsilon}_m$ can easily discriminate these "wrap-around" jumps from true variations of the time delay and therefore determine the underlying infinite range estimate and correctly compute the decision metric [4].

As a final remark, let us note that with the digital filter and square timing estimation, the planar filtering is nothing but a (weighted) summation of successive values X_m; and this is merely an extension of the estimation interval LT in the algorithm for computing X_m (Fig. 1) with an additional weighting of the terms.

V. Realization of the Detector

Fig. 8 shows a possible realization of the computation of X_m which allows high data rates through the use of parallel processing and pipelining.

With a double set of latches, the quadruples of samples belonging to an estimation interval of length $L = 1$ are collected. Since the sin and cos functions take on only values 0 and ± 1, no multiplications are necessary. The samples can then be processed at the symbol rate $1/T$ rather than at the $4/T$ sampling rate. Squaring and addition can be divided by latches into further pipeline stages. Thus, the fact that the estimation algorithm needs 4 samples per symbol (instead of one or two as other algorithms do) is relevant virtually only to the A/D converter and therefore the estimator can be used even at high data rates. We are currently incorporating the detector into a CMOS standard cell chip which will run at about 10 Mbits/s.

In cases where a low number of samples per symbol is important (e.g., when adaptive echo cancellers are used), the actual sampling rate can be reduced to 2 samples per symbol by using a simple all-pass filter to generate the missing samples [2].

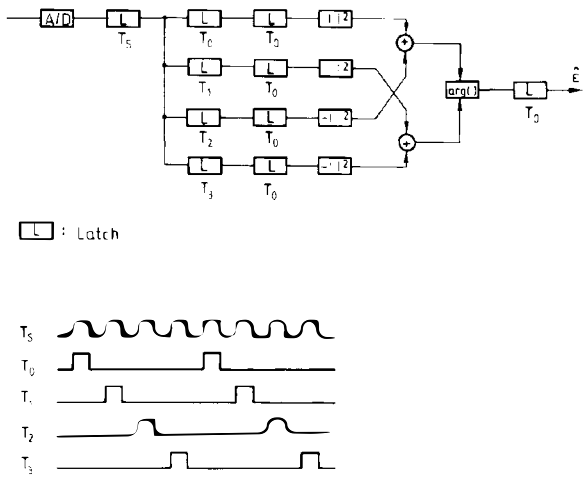

Fig. 8. Fast digital realization of the detector.

VI. Conclusions

The proposed timing recovery enables a VLSI realization of digital receivers which can operate on a sampled input signal without any feedback to the sampling device. The latter can operate at a fixed rate with a free running oscillator. The planar filtering algorithm results in very fast and hangup-free timing recovery.

Appendix A

Equivalence of discrete-time and continuous-time computation of the Fourier coefficients of periodic band-limited functions. Assuming $x(t)$ to be a T periodic and $N/2T$-band-limited signal, we show that

$$\sum_{k=k_0}^{k_0+LN-1} x(kT/N)e^{-j2\pi k/N} = \frac{LN}{T}\int_0^T x(t)e^{-j2\pi t/T}\,dt. \tag{A1}$$

To do so, we start with the integral form. Due to the low-pass limitation, we can rewrite the signal by using sinc-interpolation (sinc x = sin x/x)

$$\int_0^T x(t)e^{-j2\pi t/T}\,dt$$

$$= \int_0^T \sum_{n=-\infty}^{\infty} x(nT/N)\,\mathrm{sinc}\left(\pi\,\frac{t-nT/N}{T/N}\right) e^{-j2\pi t/T}\,dt \tag{A2}$$

$$= \sum_{k=k_0}^{k_0+N-1} x(kT/N) \sum_{m=-\infty}^{\infty} \cdot \int_0^T \mathrm{sinc}\left(\pi\,\frac{t-mT-kT/N}{T/N}\right) e^{-j2\pi t/T}\,dt \tag{A3}$$

$$= \sum_{k=k_0}^{k_0+N-1} x(kT/N)\,\mathfrak{F}\left\{\mathrm{sinc}\left(\pi\,\frac{t-kT/N}{T/N}\right)\right\}_{f=1/T} \tag{A4}$$

$$= \frac{T}{LN}\sum_{k=k_0}^{k_0+LN-1} x(kT/N)e^{-j2\pi k/N}. \tag{A5}$$

In particular, with $x(t) = \Sigma_{n=-\infty}^{\infty} y(t - nT)$, we have

$$\sum_{k=k_0}^{k_0+LN-1} x(kT/N)e^{-j2\pi k/N} = \frac{LN}{T} Y(1/T). \tag{A6}$$

Appendix B

We first compute the expectation

$$\begin{aligned} E[x_k x_{k'}] &= E\left[\left(\sum_{n_1} a_{n_1} g(kT/N - nT) + \tilde{n}(kT/N)\right)\right. \\ &\cdot \left(\sum_{n_2} a_{n_2} g(kT/N - nT) + \tilde{n}(kT/N)\right)^* \\ &\cdot \left(\sum_{n_3} a_{n_3} g(k'T/N - nT) + \tilde{n}(k'T/N)\right) \\ &\cdot \left.\left(\sum_{n_4} a_{n_4} g(k'T/N - nT) + \tilde{n}(k'T/N)\right)^*\right]. \end{aligned} \tag{B1}$$

With

$$E[a_i \tilde{n}(t)] = 0 \tag{B2}$$

$$E[a_i] = 0 \tag{B3}$$

$$E[a_i a_j^*] = \delta_{ij} \tag{B4}$$

$$E[a_i a_j] = 0 \tag{B5}$$

$$E[a_i a_j^* a_k a_l^*] = \begin{cases} 1 & \text{for } i = j \neq k = l \\ 1 & \text{for } i = l \neq j = k \\ \gamma & \text{for } i = j = k = l \\ 0 & \text{otherwise} \end{cases} \tag{B6}$$

$$E[n(t)n^*(t+\tau)] = N_0 \varphi(\tau) = N_0 \int_{-\infty}^{\infty} g_R(t) g_R^*(t+\tau)\, dt \tag{B7}$$

10 of the 16 terms which result from (B1) vanish. The following terms remain:

$$E[x_k x_{k'}] = E_1 + 2E_2 + 2E_3 + E_4 \tag{B8}$$

with

$$\begin{aligned} E_1 &= \sum_{n_1} \sum_{n_2} \sum_{n_3} \sum_{n_4} E[a_{n_1} a_{n_2}^* a_{n_3} a_{n_4}^*] \\ &\cdot g(kT/N - n_1 T) g^*(kT/N - n_2 T) \\ &\cdot g(k'T/N - n_3 T) g^*(k'T/N - n_4 T) \end{aligned} \tag{B9}$$

$$\begin{aligned} &= \sum_{i=-\infty}^{\infty} \sum_{j=-\infty}^{\infty} p_0(kT/N - iT) p_0(k'T/N - jT) && E_{11} \\ &+ \sum_{i=-\infty}^{\infty} \sum_{j=-\infty}^{\infty} p_j(kT/N - iT) p_j(k'T/N - iT) && E_{12} \\ &+ (\gamma - 2) \sum_{i=-\infty}^{\infty} p_0(kT/N - iT) p_0(k'T/N - iT) && E_{13} \end{aligned}$$

$$\begin{aligned} E_2 &= \sum_{n_1} \sum_{n_2} E[a_{n_1} a_{n_2}^*] g(kT/N - n_1 T) \\ &\cdot g^*(kT/N - n_2 T) E[n(k'T/N) n^*(k'T/N)] \\ &= N_0 \sum_{i=-\infty}^{\infty} p_0(kT/N - iT) \varphi(0) \end{aligned} \quad \text{(B1}$$

$$\begin{aligned} E_3 &= \sum_{n_1} \sum_{n_2} E[a_{n_1} a_{n_2}^*] g(kT/N - n_1 T) \\ &\cdot g^*(k'T/N - n_2 T) E[n(k'T/N) n^*(kT/N)] \\ &= N_0 \sum_{i=-\infty}^{\infty} g(kT/N - iT) g^*(k'T/N - iT) \\ &\cdot \varphi((k-k')T/N) \end{aligned} \quad \text{(B1}$$

$$\begin{aligned} E_4 &= E[n(kT/N) n^*(kT/N) n(k'T/N) n^*(k'T/N)] \\ &= N_0^2 \varphi^2(0) + N_0^2 \varphi^2((k-k')T/N). \end{aligned} \quad \text{(B1}$$

The corresponding terms in (27) are now computed. T[illegible] approximations are valid for large estimation intervals LT.

$$\begin{aligned} S_{11} &= \sum_{k=0}^{LN-1} \sum_{k'=0}^{LN-1} \sum_{i=-\infty}^{\infty} \sum_{j=-\infty}^{\infty} p_0(kT/N - iT) \\ &\cdot p_0(k'T/N - jT) \sin(2\pi k/N) \sin(2\pi k'/N) \\ &= \left[\frac{LN}{T} \operatorname{Im} P_0(1/T)\right]^2 = 0 \end{aligned} \quad \text{(B1}$$

$$\begin{aligned} S_{12} &= \sum_{k=0}^{LN-1} \sum_{k'=0}^{LN-1} \sum_{i=-\infty}^{\infty} \sum_{j=-\infty}^{\infty} p_j(kT/N - iT) \\ &\cdot p_j(k'T/N - iT) \sin(2\pi k/N) \sin(2\pi k'/N) \\ &\approx L \sum_{k=-\infty}^{\infty} \sum_{k'=-\infty}^{\infty} \sum_{j=-\infty}^{\infty} p_j(kT/N) p_j(k'T/N) \\ &\cdot \sin(2\pi k/N) \sin(2\pi k'/N) \\ &= L(N/T)^2 \sum_{j=-\infty}^{\infty} (\operatorname{Im} P_j(1/T))^2 \end{aligned} \quad \text{(B1}$$

$$\begin{aligned} S_{13} &= (\gamma - 2) \sum_{k=0}^{LN-1} \sum_{k'=0}^{LN-1} p_0(kT/N) p_0(k'T/N) \\ &\cdot \sin(2\pi k/N) \sin(2\pi k'/N) \\ &\approx (\gamma - 2) L \sum_{k=-\infty}^{\infty} \sum_{k'=-\infty}^{\infty} \sum_{i=-\infty}^{\infty} p_0(kT/N - iT) \\ &\cdot p_0(k'T/N - iT) \sin(2\pi k/N) \sin(2\pi k'/N) \\ &= L(N/T)^2 (\gamma - 2) (\operatorname{Im} P_0(1/T))^2 = 0. \end{aligned} \quad \text{(B1}$$

Therefore,

$$S_1 \approx L(N/T)^2 \sum_{j=-\infty}^{\infty} (\operatorname{Im} P_j(1/T))^2 \quad \text{(B1}$$

and

$$\begin{aligned} S_2 &= N_0 \sum_{k=0}^{LN-1} \sum_{k'=0}^{LN-1} \sum_{i=-\infty}^{\infty} p_0(kT/N - iT) \varphi(0) \\ &\cdot \sin(2\pi k/N) \sin(2\pi k'/N) = 0 \end{aligned} \quad \text{(B1}$$

$$S_3=N_0\sum_{k=0}^{LN-1}\sum_{k'=0}^{LN-1}\sum_{i=-\infty}^{\infty} g(kT/N-iT)g^*(k'T/N-iT)$$

$$\cdot\ \varphi((k-k')T/N)\sin(2\pi k/N)\sin(2\pi k'/N)$$

$$\approx LN_0\sum_{k=-\infty}^{\infty}\sum_{k'=-\infty}^{\infty} g(kT/N)g^*(k'T/N)$$

$$\cdot\ \varphi((k-k')T/N)\sin(2\pi k/N)\sin(2\pi k'/N)$$

$$\approx L(N/T)^2N_0\int_{-\infty}^{\infty}\int_{-\infty}^{\infty} g(t)g^*(t')\varphi(t-t')$$

$$\cdot\ \sin(2\pi t/T)\sin(2\pi t'/T)\,dt\,dt'$$

$$:=L(N/T)^2N_0I_3 \tag{B18}$$

$$S_4=N_0^2\sum_{k=0}^{LN-1}\sum_{k'=0}^{LN-1}(\varphi^2(0)+\varphi^2((k-k')T/N))$$

$$\cdot\ \sin(2\pi k/N)\sin(2\pi k'/N)$$

$$=N_0^2\sum_{k=0}^{LN-1}\sum_{k'=0}^{LN-1}\varphi^2((k-k')T/N)$$

$$\cdot\ \sin(2\pi k/N)\sin(2\pi k'/N)$$

$$\approx N_0^2\sum_{\substack{m=0\\(m+n)}}^{2LN-2}\sum_{\substack{n=-\infty\\ \text{even}}}^{\infty}\varphi^2(nT/N)$$

$$\cdot\ \sin\left(2\pi\frac{m+n}{2}\Big/N\right)\sin\left(2\pi\frac{m-n}{2}\Big/N\right)$$

$$=N_0^2\sum_{\substack{m=0\\(m+n)}}^{2LN-2}\sum_{\substack{n=-\infty\\ \text{even}}}^{\infty}\varphi^2(nT/N)$$

$$\cdot\ \frac{1}{2}(\cos(2\pi m/N)-\cos(2\pi n/N))$$

$$=N_0^2\sum_{n=-\infty}^{\infty}(LN/2)\varphi^2(nT/N)\cos(2\pi n/N)$$

$$\approx\frac{LN^2}{2T}N_0^2\int_{-\infty}^{\infty}\varphi^2(t)\cos(2\pi t/T)\,dt$$

$$=\frac{LN^2}{2T}N_0^2\,\mathrm{Re}\,\Psi(1/T)\qquad \text{with } \Psi(f)=\mathfrak{F}[\varphi^2(t)]. \tag{B19}$$

Finally, we can write

$$E[(\mathrm{Im}\,X)]=S_1+2S_3+S_4. \tag{B20}$$

The three terms represent the parts that are generated by (signal × signal), (signal × noise), and (noise × noise). Correspondingly, the variance of $\hat{\epsilon}$ is

$$\mathrm{var}[\hat{\epsilon}]=\sigma^2_{s\times s}+\sigma^2_{s\times n}+\sigma^2_{n\times n} \tag{B21}$$

with

$$\sigma^2_{s\times s}=\frac{1}{(2\pi)^2}\frac{L\left(\frac{N}{T}\right)^2\sum_m(\mathrm{Im}\,P_m(1/T))^2}{\left(\frac{LN}{T}P_0(1/T)\right)^2}=\frac{1}{(2\pi)^2}\frac{1}{L}\frac{\sum_m(\mathrm{Im}\,P_m(1/T))^2}{(P_0(1/T))^2} \tag{B22}$$

$$\sigma^2_{s\times n}=\frac{1}{(2\pi)^2}\frac{2L\left(\frac{N}{T}\right)^2N_0I_3}{\left(\frac{LN}{T}(P_0(1/T)\right)^2}=\frac{1}{(2\pi)^2}\frac{1}{L}N_0\frac{2I_3}{P_0(1/T))^2} \tag{B23}$$

$$\sigma^2_{n\times n}=\frac{1}{(2\pi)^2}\frac{\left(\frac{N}{T}\right)^2LTN_0^2\frac{1}{2}\mathrm{Re}\,\Psi(1/T)}{\left(\frac{LN}{T}P_0(1/T)\right)^2}=\frac{1}{(2\pi)^2}\frac{1}{L}N_0^2\frac{\frac{T}{2}\mathrm{Re}\,\Psi(1/T)}{(P_0(1/T))^2}. \tag{B24}$$

Acknowledgment

We would like to thank the reviewers for their valuable comments and suggestions.

References

[1] K. H. Mueller and M. Müller, "Timing recovery in digital synchronous data receivers," *IEEE Trans. Commun.*, vol. COM-14, pp. 516–530, May 1976.
[2] O. Agazzi, C. -P. J. Tzeng, D. G. Messerschmitt, and D. A. Hodges, "Timing recovery in digital subscriber loops," *IEEE Trans. Commun.*, vol. COM-33, pp. 558–569, June 1985.
[3] F. M. Gardner, "A BPSK/QPSK timing-error detector for sampled receivers," *IEEE Trans. Commun.*, vol. COM-34, pp. 423–429, May 1986.
[4] M. Oerder, G. Ascheid, R. Häb, and H. Meyr, "An all digital implementation of a receiver for bandwidth efficient communication," in *Signal Processing III: Theories and Applications*, I. T. Young *et al.*, Eds. New York: Elsevier, 1986, pp. 1091–1094.
[5] L. E. Franks and J. P. Bubrouski, "Statistical properties of timing jitter in a PAM timing recovery scheme," *IEEE Trans. Commun.*, vol. COM-22, pp. 913–920, July 1974.
[6] M. Moeneclaey, "Prefilter optimization for the filter and square synchronizer," *Arch. Elektr. Übertragung*, pp. 257–261, 1984.
[7] A. N. D'Andrea, U. Mengali, and M. Moro, "Nearly optimum prefiltering in clock recovery," *IEEE Trans. Commun.*, vol. COM-34, pp. 1081–1088, Nov. 1986.
[8] B. D. O. Anderson and J. B. Moore, *Optimal Filtering*. Englewood Cliffs, NJ: Prentice-Hall, 1979.

★

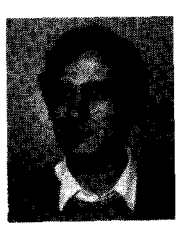

Martin Oerder (S'88) was born in Aachen, West Germany, on August 26, 1957. He received his Dipl.-Ing. degree in electrical engineering from Aachen University of Technology in 1984. Currently, he is pursuing the Ph.D. degree at Aachen University of Technology.

His interests are in the field of digital communications with emphasis on digital synchronization techniques.

Heinrich Meyr (M'75–SM'83–F'86) received the Dipl.-Ing. and Ph.D. degrees from the Swiss Federal Institute of Technology (ETH), Zurich, in 1967 and 1973, respectively.

From 1968 to 1970 he held research positions at Brown Boveri Corporation, Zurich, and the Swiss Federal Institute for Reactor Research. From 1970 to the summer of 1977 he was with Hasler Research Laboratory, Bern, Switzerland. His last position at Hasler was Manager of the Research Department. During 1974 he was a Visiting Assistant Professor with the Department of Electrical Engineering, University of Southern California, Los Angeles. Since the summer of 1977 he has been Professor of Electrical Engineering at the Aachen Technical University (RWTH), Aachen West Germany. His research focuses on synchronization, digital signa processing, and in particular, on algorithms and architectures suitable fc VLSI implementation. In this area he is frequently in demand as a consultar to industrial concerns. He has published work in various fields and journal and holds over a dozen patents.

Dr. Meyr served as a Vice Chairman for the 1978 IEEE Zurich Semina and as an International Chairman for the 1980 National Telecommunication Conference, Houston, TX. He served as Associate Editor for the IEE TRANSACTIONS ON ACOUSTICS, SPEECH, AND SIGNAL PROCESSING fror 1982 to 1985, and as Vice President for International Affairs of the IEE Communications Society.